Journal of Fluorescence, Vol. 14, No. 4, July 2004 (©2004)

Steady-State and Time-Resolved Spectroscopic Characteristics of Mesoionic Oxazolones Solutions

Marilena Vasilescu,[1,4] F. Dumitrascu,[2] H. Lemmetyinen,[3] and N. Tkachenko[3]

Received November 20, 2003; revised March 10, 2004; accepted March 10, 2004

Three new mesoionic oxazolo[3,2-b]pyridazin-2-one derivatives, in different solutions have been investigated by UV-Vis absorption, steady-state and time-resolved fluorescence methods. The effect of substituents on the extension of conjugation of the π-electrons from mesoionic oxazolone has been evidenced by bathochromic shifts of the absorption and fluorescence maxima positions. The fluorescence decay data could be fitted to single-exponential or double-exponential function. The lifetime values are much higher in aprotic polar solvents and in the case of the derivatives that present an extension of the conjugation of π-electrons. The properties of the compounds present a solvent dependence, being tested in micellar solutions as potential molecular probe "sensitive" to the environment polarity.

KEY WORDS: Mesoionic oxazolo[3,2-b]pyridazin-2-one fluorescence; fluorescence lifetime.

INTRODUCTION

Heterocycles have at least one lone pair of nonbonding *n* electrons. They can be excited into a π^* ring orbital by an electronic promotion which is commonly referred to an $n \rightarrow \pi^*$ transition. The compound, which has a lowest energy absorption band corresponding to an n–π^* transition, is generally not fluorescent, but it is fluorescent if this band corresponds to a π–π^* transition. Solutions of heterocyclic molecules, pyridine, pyrrole, furan, thiophene, and benzofuran do not fluoresce, but indole does in aqueous solutions [1,2]. Absorption and fluorescence spectra of heterocycles are very sensitive to solvent effect and hydrogen bonding plays a key role in that sensitivity.

The fluorescence of aromatic hydrocarbons generally depends on the substituent nature and position. In the case of five atom heterocycles the substituent position is critical. Indole (2,3-benzopyrrole) is fluorescent, whereas pyrrole is not fluorescent. The addition of a double bounded N atom to indole can increase or decrease the fluorescence function of the nature and position of the substituent.

The mesoionic oxazolo[3,2-b]pyridazin-2-one (known as münchnones) were prepared by cyclodehydration of *N*-alkyl-*N*–acyl α-aminoacids with reagents such as acetic anhydride, trifluoroacetic anhydride, or dicyclohexyl carbodiimide [3–9]. The münchnones are utilized *in situ* because they are too unstable to be isolated [3–9]. At the Institute of Organic Chemistry – Bucharest the isolation of more stable mesoionic oxazolo[3,2-b]pyridazin-2-one derivatives has been accomplished. These compounds exhibit an intense fluorescence.

In this study we present the spectrophotometric characterization (absorption and fluorescence) of three new mezoionic oxazolones. The UV-Vis absorption, steady state and time-resolved fluorescence measurements have been generally conducted in ethanol to evidence the effect of the substituent, but also in aprotic solvents (acetonitrile,

[1] Institute of Physical Chemistry, Romanian Academy, Splaiul Independentei, Bucharest, Romania.
[2] Centre of Organic Chemistry, Romanian Academy, Splaiul Independentei, Bucharest, Romania.
[3] Institute of Materials Chemistry, Tampere University of Technology, Tampere, Finland.
[4] To whom correspondence should be addressed at Institute of Physical Chemistry, Romanian Academy, Splaiul Independentei 202, 77208 Bucharest, Romania. E-mail: mvasilescu@chimfiz.icf.ro

1053-0509/04/0700-0443/0 © 2004 Plenum Publishing Corporation

DMSO, toluene, cyclohexane) to evidence the interaction solute-solvent.

EXPERIMENTAL

Materials and Solutions

The mesoionic oxazolo[3,2-b]pyridazin–2-one derivatives of the oxazolones have the molecular structures **I–III**, confirmed by elemental analysis, IR spectroscopy, mass and NMR spectrometry. Their synthesis and chemical properties have been communicated [12] and will be published elsewhere. Solvents (spectroscopic grade) from Merck have been used. Sodium dodecyl sulfate (SDS), especially pure grade (BDH), hexaethylene glycol monododecylether ($C_{12}E_6$) and octaethylene glycol monohexadecyl ether ($C_{16}E_8$) surfactants (from Nikko Chemicals), poly(ethylene glycol) 200 (CW) (Loba Chemie), and poly(propylene glycol), average molecular weight 2000 (Aldrich) were used without purification.

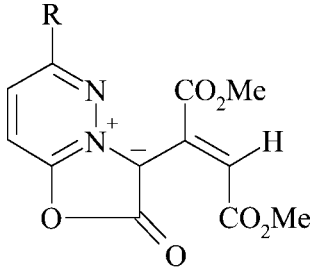

I: R = Me **II**: R = Ph

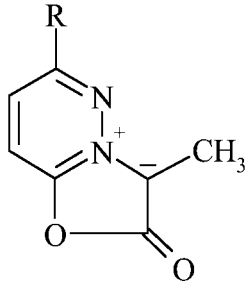

III: R = 4-ClC_6H_4

A fresh stock ethanolic solution (ca. 1 mM) was prepared for each oxazolone derivative. Appropriate amounts of stock solutions were transferred into a volumetric flask and the ethanol evaporated under a stream of nitrogen, then the solvents or aqueous surfactant solutions (3% SDS, 2% $C_{12}E_6$ and 2% $C_{16}E_8$, values above the critical micellar concentration) were added. The final concentrations of the oxazolones were in the 10^{-5} M–5×10^{-5} M range. The micellar solutions were magnetically stirred for a few hours. Solutions were kept in the dark. The study on the photochemical stability of oxazolones in different solvents has been conducted by us and the results will be published separately.

Methods

The fluorescence spectra (emission and excitation) were recorded with Spex spectrofluorimeter, at 23°C. The emission and excitation spectra were corrected. The relative fluorescence quantum yields were determinated by comparison to diluted quinine bisulfate solution in 0.1 N H_2SO_4, with 0.55 absolute quantum yield [13]. The fluorescence lifetime of oxazolones has been measured, at 21°C, using a single photon counting technique. The excitation setup uses a mode – locked Nd-YAG laser (Spectra Physics Model 379.344S) and a dye-laser. The excitation wavelength was 300 nm. The experimental method is described in [14]. Data were fitted by a monoexponential or a double-exponential function: $F(t) = a_1 \exp(-t/\tau_1) + a_2 \exp(-t/\tau_2)$.

Absorption spectra were recorded with a Shimadzu UV-VIS 2501 PC spectrophotometer, at 23°C.

RESULTS

Steady-State Spectra of Oxazolones Derivatives

Substituent Effect

The photophysical investigation of these new compounds starts with their UV-Vis absorption characterization. The UV-Vis absorption spectra of oxazolones (**I–III**) in ethanol exhibit four bands, the absorption maxima (but only wavelengths grater than 220 nm, because of the absorption of ethanol) and the molar extinction coefficients, ε, being presented in Table I. The data shown in Table I evidence the effect of substituent. By the replacement of methyl group (compound **I**) with phenyl (compound **II**) the conjugation of the π-electrons from mesoionic oxazolone is extended with the π-electrons from benzene ring. In the case of derivative **II** one can observe a bathochromic shift of $\Delta_{max} = 14$ nm for low-energy band ($S_0 \rightarrow S_1^*$ transition) and the modification of the ε values. Figure 1 shows for comparison the absorption spectra, in the 230–500 nm range. In the case of derivative **III**, the low-energy band is blue-shifted ($\Delta_{max} = 22$ nm) (see also Table I). This hypsochromic effect is assigned to the replacement of fumaryl cathene (in **II**) with the methyl group, there-

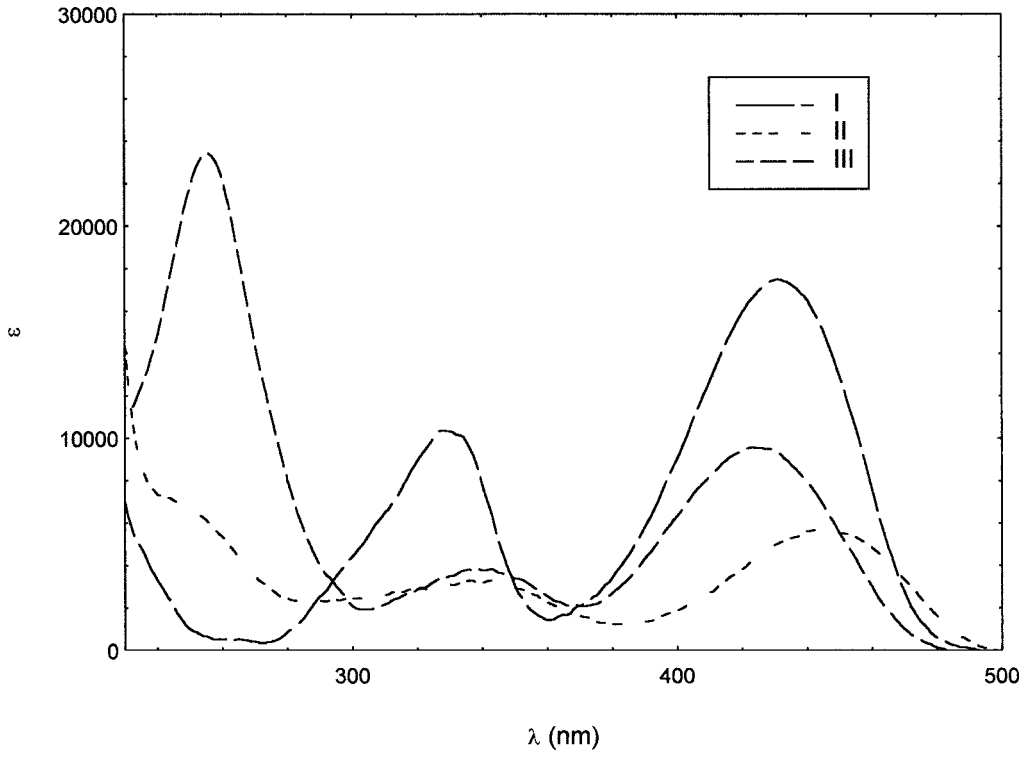

Fig. 1. The absorption spectra of the compounds **I**–**III** in ethanol.

fore the conjugation of π-electrons being shortened. For high-enegy absorption band an hyperchromic effect can be observed.

Table I also shows the positions of emission maxima (λ_{em}) in fluorescence spectra of oxazolone solutions (5×10^{-5} M) and the fluorescence quantum yield, Φ_f. As in the case of absorption, one can remark the red shift in the emission spectrum with the extension of the conjugation (compare **I** with **II**), and the blue shift in the case of **III** comparatively with **II**, but the modifications of the emission maxima are smaller. This difference of the behavior of the compound **III** on the excited states can be recover in larger Stokes shift ($\Delta\nu$) for this compound (Table I). The quantum yield of compound **I** is lowest, pointing to the role of the methyl group.

Figure 2 shows the excitation spectra of the compounds in ethanol. The positions of the excitation bands are practically the same as the positions of the absorption bands, but the long wavelength absorption band is more efficient for fluorescence excitation.

Table I. Absorption (λ_{abs} and ε), Emission (λ_{em} and Fluorescence Quantum Yield (Φ_f)) and Stokes Shift ($\Delta\nu$) of Mesoionic Oxazolones Solutions in Ethanol

Compound	λ_{abs} (nm)	ε (L·mol^{-1} cm^{-1}) $\times 10^3$	λ_{em} (nm)	$\Delta\nu$ cm^{-1}	Φ_f
I	431	17.50	488	2877	0.096
	328	10.36			
II	447	5.71	510.8	2895	0.275
	343	2.58			
	242	7.29			
III	427	8.19	508.1	3960	0.289
	343	3.27			
	255	23.45			

Solvent Effect

Representative solvents have been selected for this investigation. Tables II–IV show the absorption band maxima wavelengths in the 300–500 nm range and the corresponding molar extinction coefficients, ε, for **I, II**, and **III** in ethanol (EtOH), acetonitrile (ACN), dimethyl sulfoxide (DMSO), and toluene (TOL). Figure 3 presents the normalized absorption and emission spectra in DMSO for **I**, **II** and **III**. The outlines of the absorption spectra illustrate the presence of some shoulders due to the overlapping of the vibrational bands. For a better evidence of the modification of absorption spectra in the mentioned solvents, the spectrum has been decomposed in gaussian

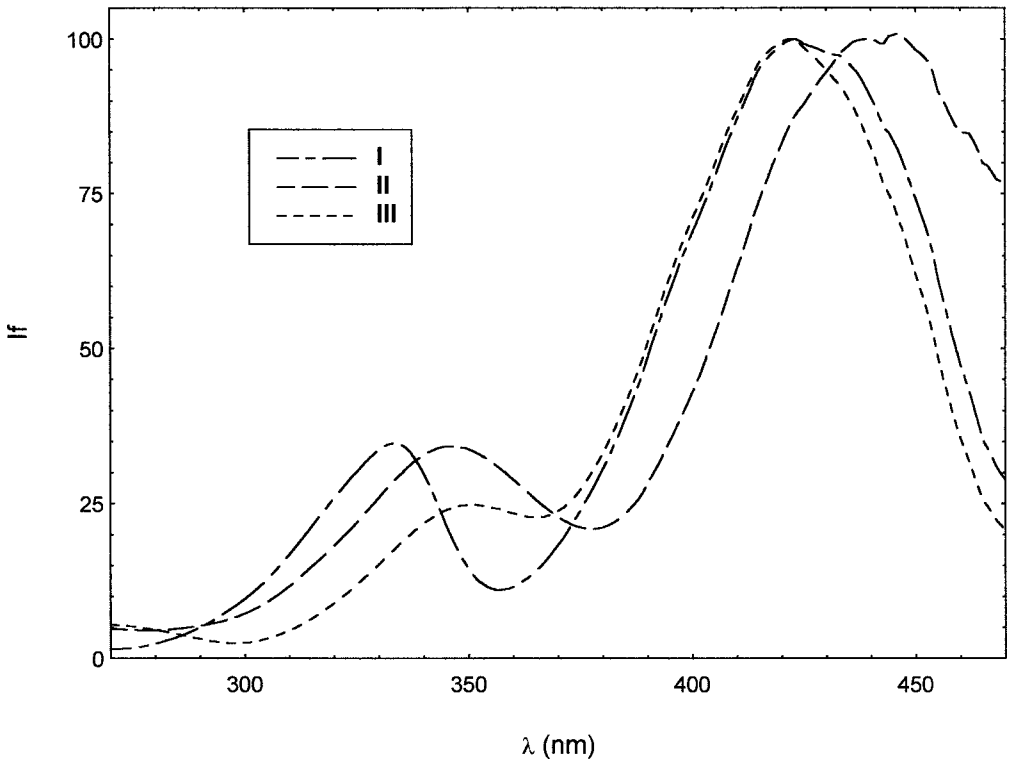

Fig. 2. The normalized excitation spectra of compounds **I–III** in ethanol, measured at $\lambda_{em} = 500$ nm.

bands using a deconvolution program, the optimal fitting of the experimental data being obtained by 6 gaussian bands summing, the number of bands being established following the values of statistical parameters of the fitting. Table IV presents the positions of the maxima and amplitudes of the gaussian bands for oxazolones in different solvents. One can thus better observe the modifications of the spectra: the increasing of the intensity and the shifts of the maxima depending on the extension of the π electrons and the solvent nature.

Toluene favors the extension of the conjugation. Tables II–IV also show the fluorescence parameters (fluorescence intensity in arbitrary units and maxima positions, λ_{em}). The fluorescence intensity is greater in DMSO probably because the compounds do not interact with the solvent. The shoulders in emission spectra of compound **III** were better positioned by decomposing the spectrum in three gaussian bands. The maximum positions and intensity (in counts per second) of these bands are mentioned in Table IV.

Table II. Absorption (λ_{max} and ε) and Fluorescence (I_f and λ_{em}) Properties of Compound **I** in Different Solutions ([**I**] $= 5 \times 10^{-5}$ M)

Solvent	λ_{max} (nm)	ε (L·mol^{-1} cm^1) $\times 10^3$	λ_{em} (nm)	I_f a.u.
EtOH	328	10.36	488.1	14
	431	17.50		
ACN	330.7	12.29	488.2	65
	434.9	20.16		
DMSO	334.4	21.77	501.8	100
	436.5	31.85		
TOL	322.1	3.95	513.5	22
	360.3	4.61		
	450.2	12.18		

Table III. Absorption (λ_{max} and ε) and Fluorescence (I_f and λ_{em}) of Compound **II** Solutions ([**II**] $= 5 \times 10^{-5}$ M)

Solvent	λ_{max} (nm)	ε (L·mol^{-1} cm^1) $\times 10^3$	λ_{em} (nm)	I_f a.u.
EtOH	242	7.29	510.8	53
	343	2.58		
	447	5.71		
ACN	359	8.32	502.0	61
	444	11.76		
DMSO	349	15.11	530.0	63
	452	30.43		
TOL	319	2.29	514.5	39
	362	2.33	548.0	
	461	6.76		

Table IV. Absorption (λ_{max} and ε (L·mol^{-1} cm^{-1})) and Fluorescence (I_f and λ_{em}) Properties of Compound **III** in Different Solutions ([**III**] $= 5 \times 10^{-5}$ M)

Solvent	λ_{max} (nm)	$\varepsilon \times 10^3$	λ_{max} (nm)	$\varepsilon \times 10^3$	I_f a.u	λ_{em} (nm)	I_f 10^6CPS	λ_{em} (nm)
EtOH	255.0	23.45	264	7.87	38	508.1	0.771	490
	343.7	3.27	267	3.09			0.991	513
	426.9	8.19	342	3.24			0.970	555
			397	2.50				
			424	7.33				
			448	2.46				
ACN	352.4	4.76	266	10.65	13	505.2	0.293	496
	433.6	10.08	325	1.80	13	529.4	0.463	529
			354	3.57			0.185	584
			397	1.93				
			423	9.06				
			453	5.81				
DMSO	270.4	11.64	269	6.39	37	525.8	0.75	503
	354.8	4.69	337	1.79			0.80	533
	436.4	10.76	353	4.44			0.78	570
			395	1.47				
			424	9.13				
			453	5.17				
TOL	283.3	0.43	286	0.39	17	501.1	0.404	497
	364.4	0.67	336	0.23	17	530.5	0.651	529
	444.8	1.38	365	0.51			0.204	584
			416	0.63				
			447	1.25				
			473	0.37				

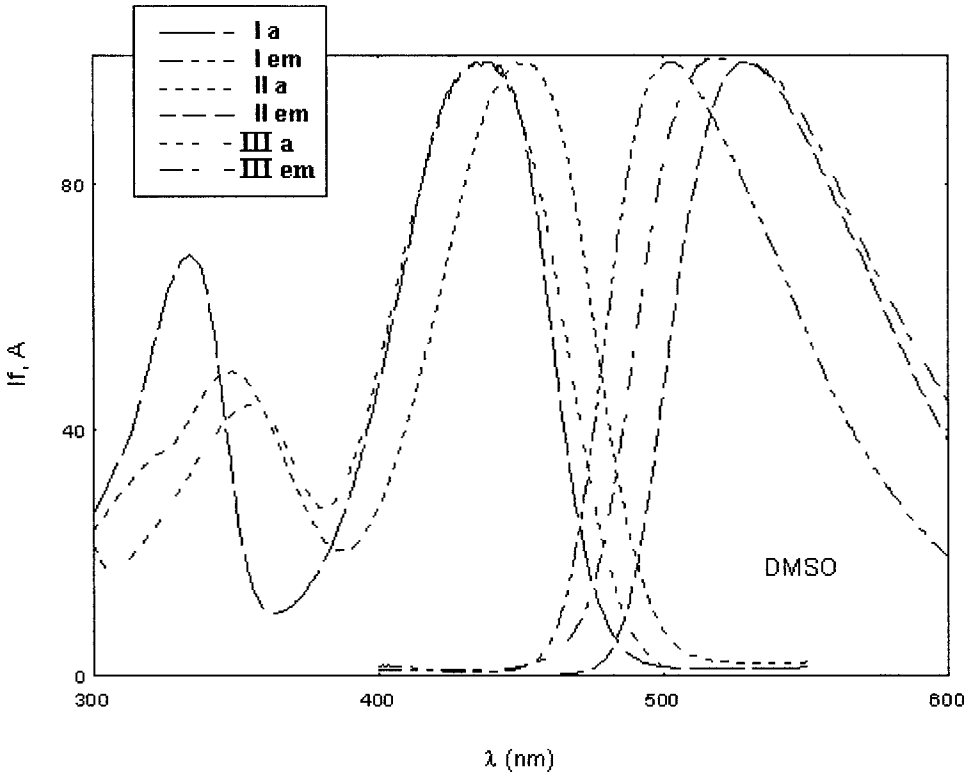

Fig. 3. The normalized absorption and emission spectra in DMSO of **I**, **II** and **III**.

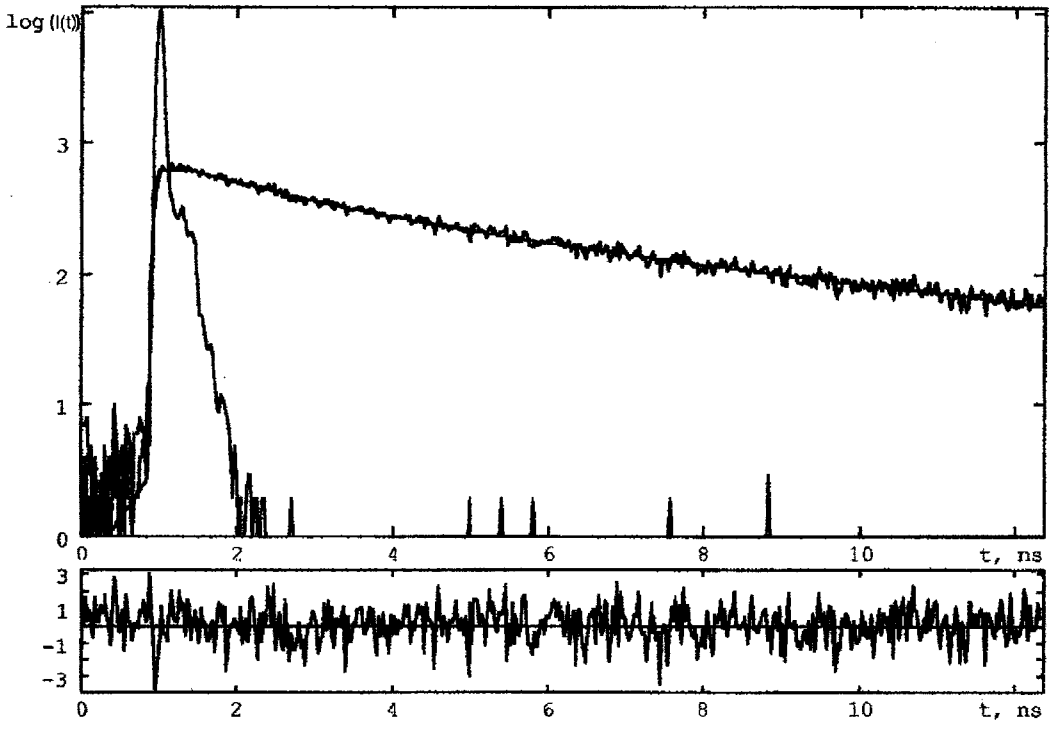

Fig. 4. The fluorescence decay curve ($\lambda_{em} = 515$ nm) of **II** in toluene and random distribution of weighted residuals ($r(t_i)$).

Fluorescence Decay

The fluorescence decay of oxazolones in all investigated solvents is measured on the nanosecond time scale. After deconvolution, a monoexponential or a biexponential decay curve is obtained (indicating in these cases that two different fluorescent conformers could be present). Figure 4 shows as an example the fluorescence decay curve ($\lambda_{em} = 515$ nm) of **II** in toluene and random distribution of weighted residuals ($r(t_i)$). The measured fluorescence lifetime values are presented in Table V. One can observe that in aprotic polar solvents the values are much higher than in a protic polar solvent (ethanol). The extension of the conjugation leads to the increase of τ values (compare **I** with **II**).

In ACN the lifetime value is highest because it contributes to the extension of the conjugation and the stability of the compound to the UV radiation during the lifetime measurement is better. The effect of EtOH is reverse. By hydrogen bonding it can perturb the extension of the conjugation, and the stability of the compounds will be lower. In the case of similar mesoionic compounds protonation takes place at the exocyclic oxygen [15] and is a ground state process. ^{15}N NMR studies on similar compounds (sydnones) have confirmed the assertion that exocyclic oxygen could be involved in formation of hydrogen bonds [16].

Oxazolones in Micellar Aqueous Solutions

The absorption and fluorescent probes are frequently used to investigate the structure of micellar solutions [17,18] or the interaction of proteins with ionic or nonionic micelles [19,20]. Because the oxazolones present

Table V. Fluorescence Lifetimes, τ, for Compounds **I**, **II** and **III**

Compound	Solvent	λ_{em} (nm)	τ (ns)	χ^2
I	EtOH	508	0.22 (55%) 1.09 (45%)	1.05
	EtOH	480	0.24 (88%) 1.09 (2%)	1.06
	Cyclohexane	480	4.53	1.05
	ACN		6.09	1.13
	DMSO	500	0.68	1.16
II	EtOH	545	0.47 (65%) 4.46 (35%)	1.11
		515	0.37 (63%) 4.24 (37%)	1.01
	ACN	510	15.02	1.09
	DMSO	529	0.80 (82%) 7.08 (18%)	1.09
	TOL	515	1.73 (56.4%) 6.58 (43.6%)	1.07
		545	1.53 (50%) 5.96 (50%)	1.07
	Chloroform	450	6.87	1.12
	CW	513	5.13	1.02
	$C_{16}E_8$	510	0.50 (65%) 4.32 (35%)	1.13
	$C_{12}E_6$	510	1.05 (56%) 10.01 (44%)	1.19
III	EtOH	500	0.26 (1%) 3.15 (99%)	1.11
	ACN	510	18.88	1.04
	DMSO	530	2.40 (78%) 5.52 (22%)	1.14
	TOL	540	3.20	1.07

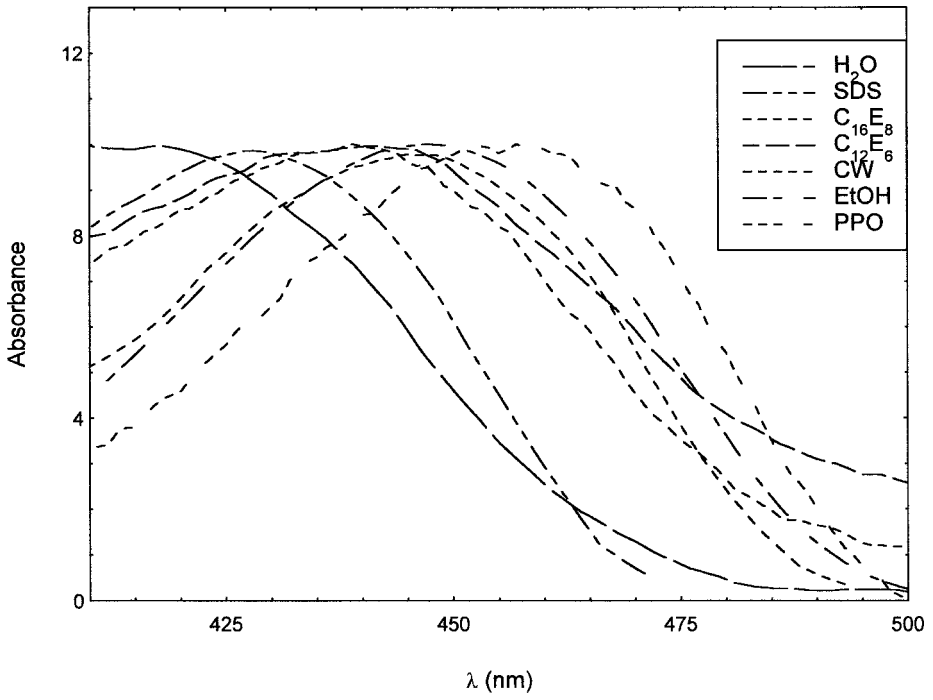

Fig. 5. Normalized absorption spectra (low-energy band) of **II** in various environments.

solvatochromic properties, the applicability of these compounds as molecular probes in micellar aqueous solutions has been investigated. CW has been selected as solvent because it reproduces the polar part of the non-ionic micelles $C_{12}E_6$ and $C_{16}E_8$, and PPO as hydrophobic medium. Absorption spectra of the compound **II** in SDS, $C_{12}E_6$ and $C_{16}E_8$ micellar solutions and in water, CW, methanol and polypropylene glycol (PPO) are presented in Figure 5. One can observe that in SDS (anionic surfactant) micelles, there is a noticeable red shift in absorption maxima, compared with water, **II** experiences a polarity between water and methanol. Some of the molecules rest probably in water, but the others are bounded to micellar surface by coulombic interaction. In non-ionic surfactants $C_{12}E_6$ and $C_{16}E_8$ micellar solutions, the spectral parameters of **II** are close to those in CW. The solubility in water is very low and therefore the oxazolone molecules prefer a more hydrophobic environment, being solubilised near the oxyethylenic-hydrated chains of the surfactant.

One can observe from Table VI that relative quantum yields (calculated considering the aria of fluorescence band and absorbance at 365 nm), are greater for **II** in ACN, PPO and SDS, and comparable for hydrophilic environments: CW, ethanol, $C_{12}E_6$ and $C_{16}E_8$. The fluorescence lifetime in $C_{12}E_6$ micelle is higher than in $C_{16}E_8$ (Table V) because of the longer ethylenic chain in $C_{16}E_8$, that is a higher hydrophilicity in the solublity zone.

Table VI. Absorption (Lowest Energy Band), Fluorescence Emission Maxima, Stokes Shift, and Relative Fluorescence Quantum Yields of **II** in Various Solvents and Micelles

Solution	λ_{max} (nm)	λ_{em} (nm)	$\Delta\nu$ (cm^{-1})	Φ_f
Water	422	436.6	792	0.229
EtOH	447	510.8	2779	0.275
CW	450	501.0	2262	0.213
ACN	444	502.0	2602	0.357
PPO	458	505.1	2033	0.538
SDS	438	457.2	959	0.298
$C_{12}E_6$	450	500.0	2222	0.231
$C_{16}E_8$	448	503.0	2440	0.222

CONCLUSIONS

The absorption spectra and steady-state fluorescence of three new mesoionic oxazolone derivatives in different solutions have been measured. The absorption spectra of **II** have evidenced bathochromic shifts because the conjugation of the π-electrons from mesoionic oxazolone is extended with the π-electrons from benzene ring. The fluorescence spectra present the same behavior. In the case of derivative **III**, the hypsochromic shift of the spectra, compared with **II** is due to the fumaryl cathene contribution to

the extension of the conjugation of the π-electrons from mesoionic oxazolone.

The fluorescence decay data could be fitted to a mono- or double-exponential function. The fluorescence lifetime values are much higher in aprotic polar solvents and are higher for **II** and **III** derivatives that present an extension of the conjugation of π-electrons.

The spectroscopic properties of the compounds present a solvent dependence. This is why **II** has been tested in micellar solutions as a potential molecular probe "sensitive" to polarity of the environment.

ACKNOWLEDGMENTS

This contribution has been financed by Romanian Academy and by a CERES grant (31/12.11.2002). Most of the fluorescence and absorption data have been obtained thanks to a co-operation program between the Romanian Academy and the Academy of Finland.

REFERENCES

1. T. Adler (1962). *Anal. Chem*. **34**, 685.
2. J. Birks and A. Cameron (1959). *Proc. Roy. Soc*. **249**, 207.
3. H. O. Bayer, R. Huisgen, R. Knorr, and F. C. Schafer (1970). *Chem. Ber.* **103**, 2581–2597.
4. W. Baker and W. D. Ollis (1957). *Quart. Rev.* **11**, 15.
5. C. A. Ramsden (1979). In D. H. R. Barton and W. D. Ollis (Eds.), *Comprehensive Organic Chemistry*, *Vol. 4*, Pergamon Press, Oxford, p. 1171.
6. C. G. Newton and C. A. Ramsden (1982). *Tetrahedron* **38**, 2965.
7. B. P. Coppola, M. C. Noe, D. J. Schwartz, R. L. Abdon, and B. M. Trost (1994). *Tetrahedron* **50**, 93–116.
8. F. Clerici, M. L. Gelmi, and P. Trimarco (1998). *Tetrahedron* **54**, 5763.
9. B. F. Lira, P. F. de Athayde Filho, J. Miller, A. Mayall Simas, A. de Farias Dias, and M. J. Vieira (2002). *Molecules* **7**, 791.
10. W. D. Ollis and C. A. Ramsden (1976). *Adv. Heterocycl. Chem.* **19**, 3–122.
11. M. B. Oliveira, J. Miller, A. B. Pereira, S. E. Galembeck, G. L. Moura, and A. M. Simas (1996). *Phosphorus, Sulfur, Silicon Relat. Elem.* **108**, 75–84.
12. F. Dumitrascu, C. Mitan, D. Dumitrescu, C. Draghici, M. T. Caproiu, and M. Vasilescu, (2003). *10-th Blue Danube Symposium on Heterocyclic Chemstry*, Vienna, Austria, September 3–6, 2003, PO-126.
13. W. H. Melhuish (1961). *J. Phys Chem*, **65**, 229.
14. H. Caldararu, A. Caragheorgheopol, M. Vasilescu, I. Dragutan, and H. Lemmetyinen (1994). *J. Phys. Chem. B*, **98**, 5320.
15. M. Ohta and H. Kato (1969). In J. P. Snyder (Ed.), Nonbenzenoid Aromatics, Academic Press, New York, pp. 117–248.
16. L. Stefaniak, M. Witanowski, B. Kamienski, and G. A. Webb (1980). *Organ. Magn. Reson.* **13**(4), 274.
17. M. Vasilescu, A. Caragheorgheopol, and H. Caldararu (2001). *Adv. Colloid Interface Sci.* **89–90**, 169.
18. M. Vasilescu, D. Anghel, M. Almgren, P. Hansson, and S. Saito (1997). *Langmuir* **13**, 6951.
19. M. Vasilescu, D. Angelescu, M. Almgren, and A. Valstar (1999). *Langmuir* **15**, 2635.
20. A. Valstar, M. Vasilescu, and M. Almgren (2001). *Langmuir* **17**, 3208.